Frequency and Spatial Variability of European Record Floods

(Article begins on next page)

19 February 2025

AGU ADVANCING EARTH AND SPACE SCIENCES

Water Resources Research®

Frequency and Spatial Variability of European Record Floods

M. Bertola[1] 🅾, **A. Castellarin[2]** 🅾, **A. Viglione[3]** 🅾, **E. Valtancoli[2]**, and **G. Blöschl[1]**

[1]Institute of Hydraulic Engineering and Water Resources Management, Technische Universität Wien, Vienna, Austria, [2]Department of Civil, Chemical, Environmental and Materials Engineering (DICAM), University of Bologna, Bologna, Italy, [3]Department of Environment, Land and Infrastructure Engineering (DIATI), Politecnico di Torino, Turin, Italy

Abstract Regional envelope curves (RECs) have been used to characterize the flooding potential of regions worldwide. However, a comprehensive assessment for Europe is still missing. In this study we use the largest European flood database to quantify the magnitude of record floods, their dependence on catchment size, and the amount of available independent information, which is needed for estimatinig the REC's exceedance probability. We propose a framework for estimating REC parameters across large areas, consisting in partitioning the domain according to the observation density and estimating the REC slope through quantile regression. The results show that the REC parameters vary substantially across Europe. The envelope unit flood associated with a catchment area of 1,000 km² varies between 0.1 and 6 m³s⁻¹ km⁻² and is highest in Mediterranean and Alpine areas and lowest in central-eastern Europe. The slope of the envelope varies between 0 and −1 and is larger in Southern Europe than in Northern Europe. These differences are explained by steeper landscape in mountaineous regions and localized short duration storms producing large floods in small catchments in the Mediterranean, whose intensities are larger than in other parts of Europe. Based on the framework of probabilistic envelope curves we show that, despite the uneven observation density, the obtained RECs are associated with comparable exceedance probabilities.

1. Introduction

Floods are ranked among the first natural hazards in terms of economic losses in Europe, the US, and worldwide (Amadio et al., 2019; Carisi et al., 2018). Global economic losses have shown a dramatic and monotonically increasing trend in the last 5 decades, even though during the same time span the frequency and magnitude of flood events may exhibit upward or downward trends, depending on the geographical area and the spatial scale being considered (Merz et al., 2021; Slater et al., 2021). In particular, recent analyses of available European annual flood sequences and relevant climatic drivers clearly illustrated that the flood frequency regime, and its changes and seasonal shifts, show complex spatial patterns (Bloschl et al., 2017, 2019), which may strongly depend on the magnitude of the flood event being considered (Bertola et al., 2020, 2021). Consequently, identifying accurate and quantitative methods for characterizing flooding potential across large and morphologically and climatically heterogeneous geographical regions is a task of paramount importance that addresses the operational needs for transboundary and international flood risk management, as advocated in Europe by the "Floods Directive" (European Union, 2007).

Among flood events, large and very large events ("megafloods") have devastating consequences and may still cause numerous fatalities together with vast economic losses in countries with a long tradition in flood risk assessment, management, and mitigation. The catastrophic July 2021 events in Western and Central Europe are a recent and drastic example of how devastating large inundation events can be, producing an overall economic loss that has been estimated in at least 11 billion of 2021 Euros in Belgium, and killing more than 220 people across Europe, including at least 184 people in Germany alone (Fekete & Sandholz, 2021; Gathen et al., 2022). Megafloods are often indicated as unpredictable events, that is events that are far beyond our prediction capabilities. Bertola et al. (2023) clearly point out that in many cases magnitude of past "surprising" European megafloods could have been anticipated based-on flood data collected up to that moment if (a) an international flood catalog would have been existing and accessible to State Members (i.e., importance of data and knowledge sharing at supranational level) and (b) the search for hydrological analogs would have been performed across large and very large spatial scales (i.e., importance of going above and beyond national studies by analyzing patterns in space across countries and watershed divides). Bertola et al. (2023)

also show that there is no need for sophisticated and complex approaches for anticipating observed megafloods, in fact, they resorted to a very classical hydrological tool, that is the regional envelopes of flood flows (see e.g. Fuller, 1914; Jarvis, 1926).

Regional envelope curves of flood flows effectively, quantitatively, and concisely summarize the flooding potential in a geographical region through a single graphical object. The traditional and most common approach for constructing a regional envelope curve is to plot the log-transformed unit flood of record (i.e., largest observed value in a flood sequence standardised by catchment area) for all gauged catchments in a given region against the logarithm of the corresponding drainage areas, and then to represent the linear upper bound of all points in the diagram (see e.g. Castellarin et al., 2005). Numerous early examples of national envelope curves of flood flows can be found in the scientific literature of the 1900s (see e.g. Jarvis, 1926 and later on Crippen & Bue, 1977 for the conterminous United States; Marchetti, 1955 for Italy; Mimikou, 1984 for Western Greece). Nevertheless, the traditional deterministic interpretation of the curves dictated the decline in their popularity once at-site and regional flood frequency analysis became standard practice in hydrology for flood hazard assessment (Dalrymple, 1960; Gumbel, 1941).

Castellarin et al. (2005) proposed a probabilistic interpretation of regional envelope curves of flood flows, showing the value of such interpretation for predicting low-frequency floods in ungauged basins (Castellarin, 2007; Castellarin et al., 2007), or for improving the robustness of regional flood frequency models (Guse et al., 2010) and suggesting potential applications also to the prediction of extreme rainstorms (Castellarin et al., 2009; Viglione et al., 2012). Nevertheless, the standard procedure for constructing the curves summarized above, as well as regression-based alternatives, is often driven by a few extreme observations, which might limit the stability of the identified upper bounds, meaning highly uncertain slope and intercept terms of the log-log linear relationship used for representing the regional envelope. Amponsah et al. (2020) focused on flash-flood events in Europe and the Mediterranean region and, to address this stability issue, they proposed Quantile Regression (QR) for identifying envelope curves. They showed that the slope has a limited variability and quantified its uncertainty.

The objective of this study is to assess the magnitude of record floods, their dependence on the catchment area and the associated exceedance probability across the entire European contient in a consistent and objective way. Our study focuses on the construction and utilisation of RECs of flood flows addressing three specific scientific and technical gaps existing in the literature, which can be summarized as follows: (a) The need for a reference method for constructing envelope curves that enables stable and comparable estimates of the expected megaflood magnitudes in different hydroclimatic regions of the World; (b) a lack of studies addressing a quantitative characterization of flooding potential and expected magnitude of severe flood events (megafloods) across Europe; (c) absence of a comprehensive study assessing the exceedance probability of the largest observed European floods as done in other areas of the World (e.g., see Douglas & Vogel, 2006 for US). More specifically, our study focuses on a comprehensive, updated (to the year 2021) and extremely rich European flood database and proposes an objective approach to the construction of envelope curves of flood flows that is not sensitive to single outliers and to the density of observations. With the proposed approach we analyze the spatial variability of the parameters of the envelope curves across the entire European continent. The results show the flooding potential of European regions in terms of the magnitude of record floods and their dependence on the catchment area. The regional differences are interpreted in terms of dominant flood generating mechanisms. We finally attach a probabilistic statement to European envelope curves, quantifying the frequency of the flood of records in space as a function of stream-gauging station density, station-years of data and spatial correlation among flood sequences.

2. Methods

2.1. Flood Data

In this study we analyze the most recent version of the European Flood Database (Bertola et al., 2023; Blöschl et al., 2019). The data set consists of annual maximum discharge series for 8,023 stream gauges in 33 European countries. The location of the stream gauges is shown in Figure 1a. The length of the series varies across the gauges, from a minimum of 10 up to a maximum of 215 years, and the median length is 51 years. The observations in the data set span from 1805 to 2021, with most observations being in the period 1961–2018.
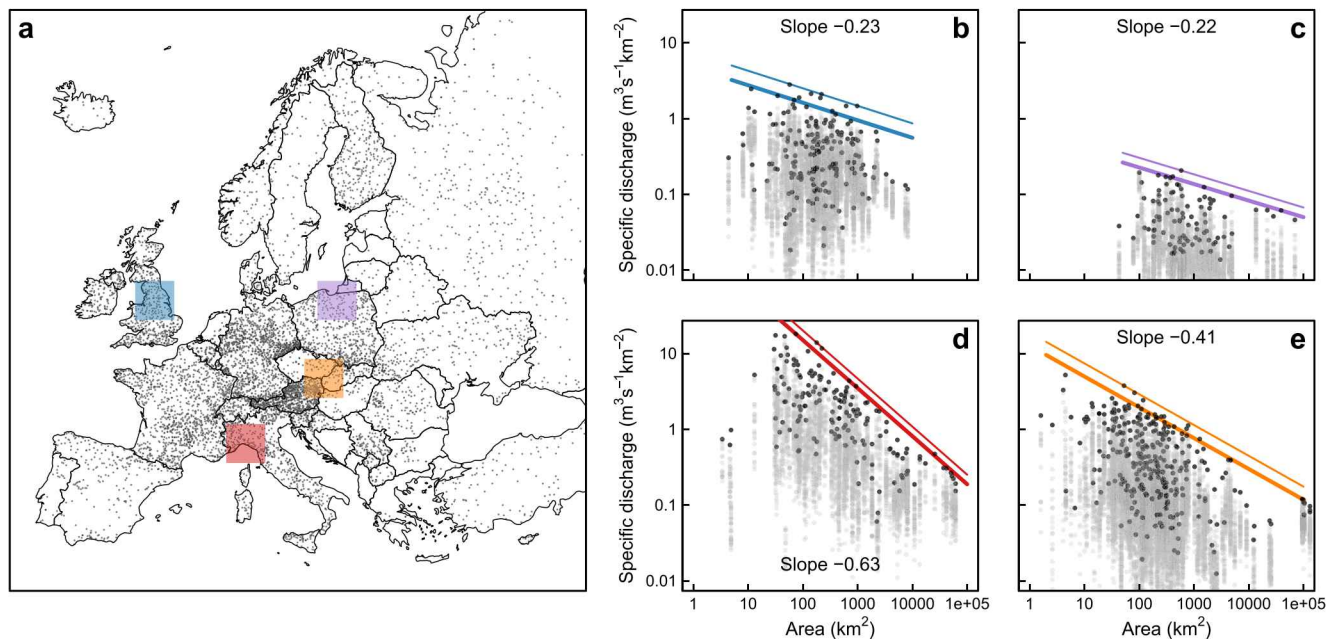
Figure 1. (a) Location of stream gauges in the European Flood Database (dots) and four example regions indicated with colored squares. (b–e) Quasi-envelope curves (thick lines) obtained with Quantile Regression with $z = 0.999$ and Regional envelope curves (RECs) (thin lines). Colors of the lines refer to the four regions of (a). Gray dots indicate specific discharges and black dots the specific floods of record. The REC slope is indicated in the panels.

The data set contains several nested catchments which could represent redundant information. We identified redundant catchment according to the guidelines in Parrett et al. (2011) and Farmer et al. (2019), which are based on the normalized distances between catchment centroids and their overlapping area, and repeated the analyses using the non-redundant catchments only (see in Supporting Information S1). We found that about 18.2% of the total can be considered redundant but, since the study focuses on the largest observations in the records, they have little effect on the results. For this reason and because removing nested catchments could imply the risk of missing some record floods, we carried out the analyses on the complete database.

2.2. Regional Envelope Curves

The Regional Envelope Curve (REC) of flood flows represents the upper bound of the specific flood of record q_{SFOR} experienced in a region, as a function of the drainage area A. The REC is defined by:

$$\log(q_{\mathrm{SFOR}}) = a + b \cdot \log(A). \tag{1}$$

The slope b is typically estimated by a regression of the unit index flood against the drainage area for all sites in the region (see e.g. Guse et al., 2010), and the intercept is determined as the minimum such that the REC bounds all unit floods of record. Amponsah et al. (2020) proposed an approach to objectively estimate the parameters of the REC for flash floods using QR, which is not sensitive to single outliers when analyzing the extremes of a data set. Their approach consists in choosing a sufficiently high quantile z for the QR, such that the estimated curve is exceeded by less than one data-point, therefore a close approximation to the REC. They suggested to set $z = (N - 0.5)/N$, where N is the number of observations in the region.

In this work, we used QR to estimate the slope b of the REC and we assessed its sensitivity to the choice of the quantile z. We tested a range of z, including $z = 0.99$, $z = 0.999$ and $z = (N - 0.5)/N$, for squared regions across all Europe of size 150, 300 and 600 km containing at least 1,000 observations. After visual inspection of the RECs, we selected $z = 0.999$ as the quantile for the QR that returns the most stable estimates of b for all the analyzed regions, while higher quantiles resulted in slopes that vary highly in space due to outliers in the data. The curve estimated with QR with $z = 0.999$ is here referred to as "quasi-envelope curve" (qREC). The REC was then obtained by shifting upwards the quasi-envelope curve until it bounds all the unit floods of record in the region. This procedure is shown in Figures 1b–1e for four regions in Europe. The specific discharges determined by the

two curves for the representative catchment area of 1,000 km^2 are named "quasi-envelope flood" and "envelope flood" for the qREC and for the REC, respectively.

The dependence of unit peak discharge on catchment area has been largely investigated and empirical evidence suggests that the slope of RECs typically ranges from -0.2 to -0.7 (Creager et al., 1966). Studies about European floods estimated the slope equal to -0.57 (Herschy, 2002) and -0.4 for flash floods (Gaume et al., 2009; Marchi et al., 2010). The attenuation of unit peak discharge with catchment area is due to several factors, including the areal reduction of precipitation depth and the flood wave attenuation during the routing. The slope of the REC also reflects the different dominant flood generating processes for different catchment scales. Figures 1b–1e clearly shows that the slope of RECs varies substantially across the four example regions in Europe, from -0.22 (Figure 1c) to -0.63 (Figure 1d). The envelope flood also varies substantially in the different regions ranging from 0.2 m^{3}s^{-1} km^{-2} (Figure 1c) to 4.8 m^{3}s^{-1} km^{-2} (Figure 1d).

Studies exist that use different REC relationships for small and large catchments (e.g., Herschy, 2002 for catchment areas <100 km^2 and >100 km^2), especially when flash-floods are of interest. Since flash floods are not captured by this flood database and most catchments in the database have areas between 102 and 1,035 km^2, we adopt here a single linear relationship in the log-log space, in line with what done by most studies in the literature.

2.3. Probabilistic Interpretation of Regional Envelope Curves

Castellarin et al. (2005) proposed a probabilistic interpretation of RECs of flood flows based on the simplifying assumptions that the flood frequency in the study region follows a single dimensionless parent distribution (i.e., index-flood hypothesis, see Dalrymple, 1960) and that a simple linear scaling law holds between the logarithms of the catchment area and annual flood adopted by the authors as the index-flood approach. Under these hypotheses, the authors demonstrate that any given envelope curve is associated with a single exceedance probability. They indicated with p the exceedance probability of the expected REC, that is the envelope curve that, on average, is expected to bound the flooding experience for a region of given characteristics (i.e., number of annual sequences, length of the sequences, and mean intersite correlation), and showed through a series of Monte Carlo simulation experiments how p is impacted by the spatial correlation between annual flood sequences. The authors then resorted to the classical concept of regional equivalent information content (see e.g. Matalas & Langbein, 1962; Stedinger, 1983) and proposed an empirical estimator of the equivalent number of independent annual sequences $\hat{M}_{EC} \leq M$, in a region with M equally-lengthed, and cross-correlated annual sequences with length n years, to be used for estimating p. The proposed empirical estimator requires the representation of the spatial (or intersite) correlation in the study region through a suitable cross-correlation formula, such as the one proposed by Tasker and Stedinger (1989):

$$\rho_{i,j} = \exp\left(-\frac{\lambda_1 \cdot d_{i,j}}{1 + \lambda_2 \cdot d_{i,j}}\right) \tag{2}$$

where $\rho_{i,j}$ and $d_{i,j}$ are the intersite correlation coefficient and distance d between the catchment centroids of sites i and j, respectively, while $\lambda_1 > 0$ and $\lambda_2 \geq 0$ are regional parameters.

Castellarin (2007) adapted the estimator $\hat{M}_{EC}$ proposed in Castellarin et al. (2005) presenting an algorithm to compute the overall effective sample years of data η_{eff}, that is the equivalent number of statistically independent annual maxima, in a real-world regional data set consisting of M cross-correlated AMS that globally spans n years, but for which the annual flood sequences are not necessarily equally-lengthed (due to e.g. presence of missing values, sensors installed/dismissed in different years, etc.). The exceedance probability p is then estimated using the Hazen plotting position formula, here expressed in terms of equivalent return period T_{EC}:

$$T_{EC} = 2 \cdot \eta_{eff} \tag{3}$$

We apply the algorithm proposed in Castellarin (2007) to the European data set of annual floods for assessing the equivalent information content of each grid pixel, that is the equivalent number of uncorrelated annual maximum discharge values, using the R-package pREC (https://github.com/alessio-pugliese/pREC.git). In particular, we compute sample correlation coefficients for all pairs of annual flood sequences having at least 50 years of paired observations and a maximum distance between catchment centroids of 1,330 km. This
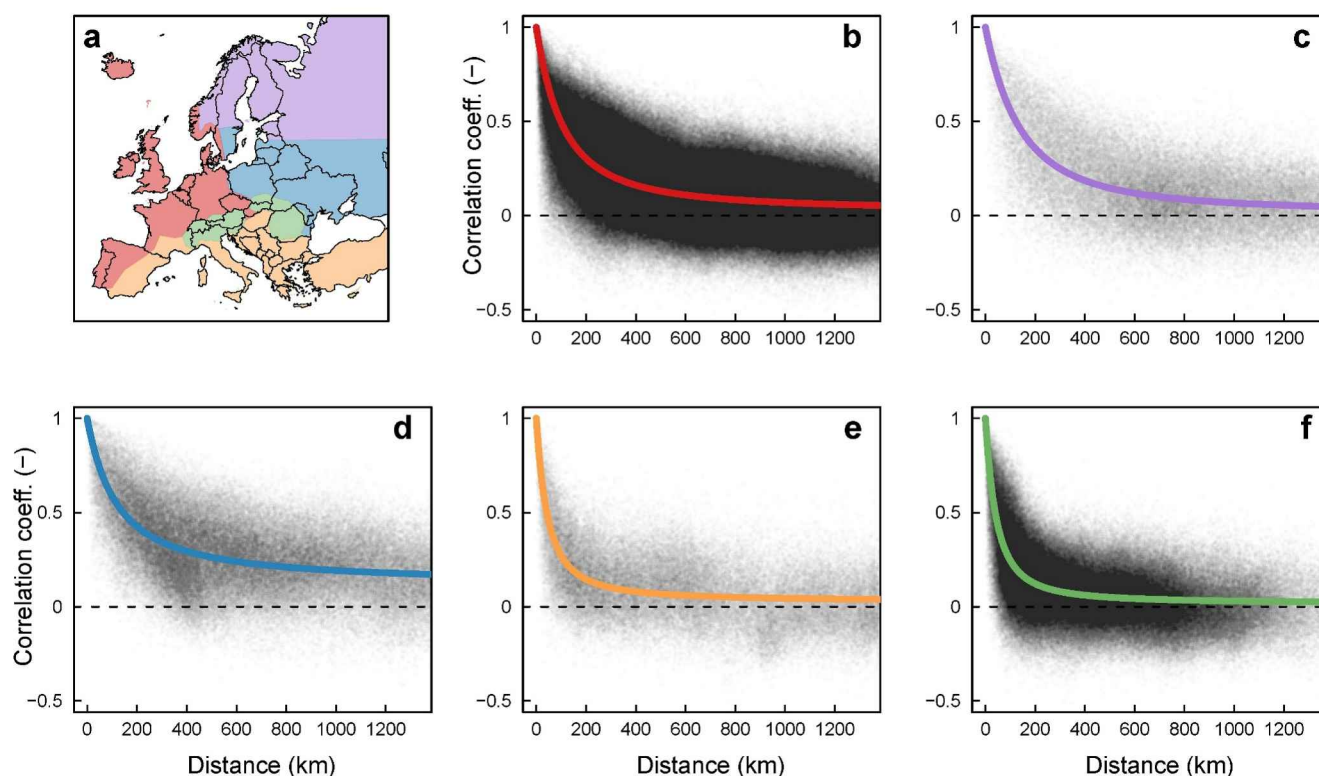
Figure 2. Spatial correlation (b–f) among annual flood sequences in 5 the hydroclimatic regions of Lun et al. (2021) in Europe: (b) Atlantic, (c) North-Eastern, (d) Central-Eastern, (e) Mediterranean and (f) Alpine. The map of the five hydroclimatic regionsis shown in panel (a). Empirical cross-correlation coefficients are illustrated as scatterplot for distances between centroids of pairs of catchments ranging from 0 to 1,330 km. The colored lines in panel (b–f) illustrates the model proposed by Tasker and Stedinger (1989) fitted to the European data set.

distance is the largest distance between pairs of catchment centroids in the grids of Section 2.4. We identify five correlation formulas for the five hydroclimatic regions of Lun et al. (2021) by estimating the parameters λ_1 and λ_2 of the Tasker and Stedinger (1989) model by using a weighted least squares optimization procedure that weights each empirical cross-correlation coefficient between two sequences proportionally to the number of paired annual maxima of the two sequences (see Castellarin, 2007). The choice of the correlation model above may have an influence the estimate of the effective number of observations. However, given the continental scale of this study and the large number of observations, we expect it to have little influence on this estimate.

Figure 2 illustrates the sample correlation coefficients together with the Tasker and Stedinger (1989) model fitted to the European data set; the estimated parameters λ_1 and λ_2 in Table 1 are consistent with the values reported in Castellarin (2007) and the definitely smaller study region analyzed therein. The spatial correlation models identified in this study indicate that the cross correlation rapidly decreases with the centroid distance in the Alpine and Mediterranean regions (Figures 2e and 2f). The cross-correlation decays less rapidly in the Atlantic and North-Eastern regions (Figures 2b and 2c) and it is highest in the Central-Eastern region (Figure 2d).

2.4. Grids

To estimate and represent the parameters of RECs for Europe, we subdivide the study domain into tiles of different size (i.e., 50, 100, 200 and 400 km) in different areas of Europe, as shown in Figure 3a. The size of the tiles is chosen such that each tile contains a reasonable number of observations. The procedure used to identify the tiles is summarized in the following.

Table 1
Parameters λ_1 and λ_2 of the Cross-Correlation Formula in Equation 2 for Five Hydroclimatic Regions

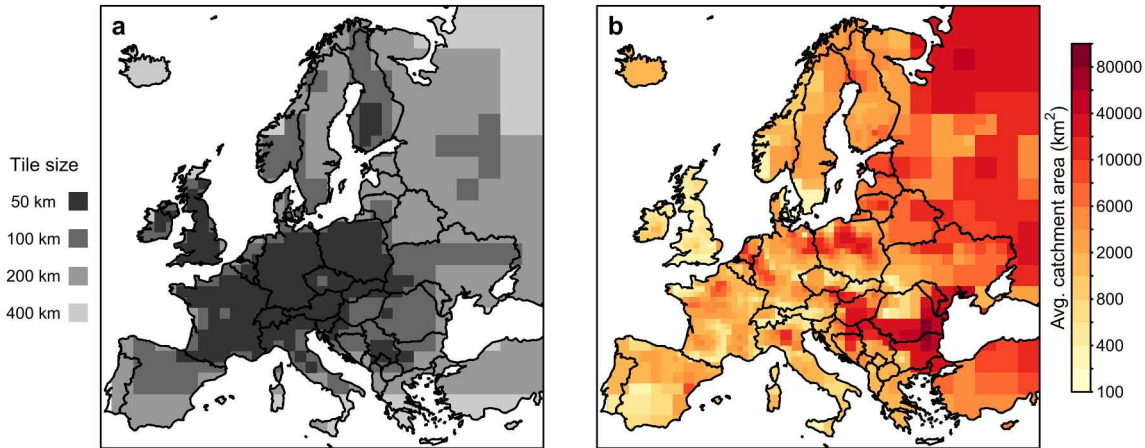| Region	λ_1 (km^{-1})	λ_2 (km^{-1})
Atlantic	0.00863	0.00224
North-eastern	0.00667	0.00148
Central-eastern	0.00708	0.00330
Mediterranean	0.02029	0.00554
Alpine	0.02119	0.00509

Figure 3. (a) Map of combined tiles with size 50, 100, 200 and 400 km. Tiles of different sizes do not overlap. (b) Average catchment area of catchments with outlets within tiles in panel (a).

- The study domain is subdivided into grids of size 50, 100, 200 and 400 km. Each grid-cell corresponds to exactly four cells in the next grid with finer resolution.
- In each grid-cell we estimate the parameters of the REC as in 2.2, using the data of the stream gauges within the cell and its six neighboring cells. Cells associated with less than 1,000 data-points were discarded.
- We repeat this procedure for the four grid-sizes and plot the results for the four grids on top of each other, with the finest grid at the top. We do not allow for partial overlap of grid-cells of different size, that is, four neighboring cells are considered only if all of them are associated with at least 1,000 data-points, otherwise the corresponding cell at the next larger size is shown entirely.

The resulting map of combined tile size is shown in Figure 3a and it reflects the heterogeneous density of available stream gauges and observations over Europe. Figure 3b shows the average area of the catchments associated with each tile.

3. Results and Discussion

Figure 4 shows maps of quasi-envelope flood and the envelope flood for Europe, that is, the specific discharges corresponding to the qREC and REC for hypothetical catchments of 1,000 km^2 of size. Specific record flood discharges are highest in the Mediterranean and Alpine regions (darker colors in Figure 4) and lowest in the parts
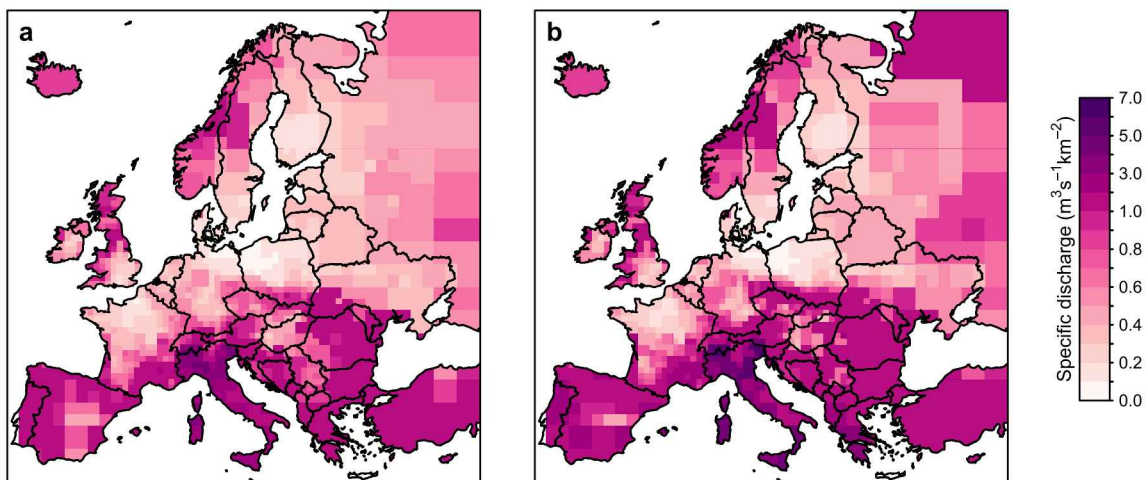

Figure 4. Map of the (a) quasi-envelope flood and (b) envelope flood in Europe for a representative catchment size of 1,000 km^2. The colors refer to specific discharges in $m^3 s^{-1} km^{-2}$ for tiles of different sizes. The size of the tiles is shown in Figure 3a.
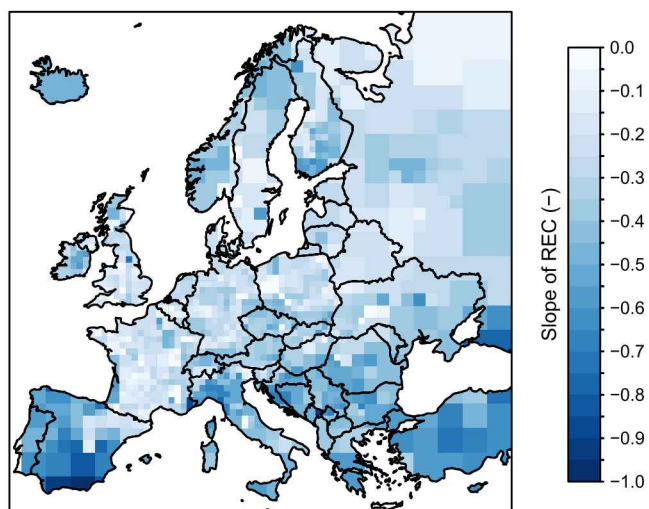
Figure 5. Map of slope of regional envelope curves indicated with colors for tiles of different sizes. The size of the tiles is shown in Figure 3a.

of the Central-Eastern and Atlantic regions. Envelope (Figure 4b) and quasi-envelope floods (Figure 4a) show similar spatial patterns. They are generally larger in southern Europe than in northern Europe, with the largest values in northern Italy (up to 3–6 m^3s^{-1} km^{-2}) and the smallest values in the Polish planes (0.1 m^3s^{-1} km^{-2}).

These spatial patterns are likely due to the different atmospheric and hydrological processes. In the Mediterranean area, especially in Italy, catchments are relatively small and flood peaks are caused by short duration storms whose intensities are larger than in other parts of Europe. Also, in mountainous regions, shallow soils and steeper landscape determine larger and peakier hydrographs than in flat regions. For these reasons, it is not surprising that colors in Figure 4 are darker in the Mediterranean area, especially in mountainous zones. This is the case for both the quasi-envelope flood (Figure 4a) and the envelope flood (Figure 4b), however this latter is slightly larger and shows less regular patterns. This is because the envelope floods are set by the largest regional record, that is, one single event sets the "level" of the envelope curve and individual outliers may result in darker patches in Figure 4b. The quasi-envelope floods (Figure 4a) are instead set through the QR, accounting for all annual maximum events, and are therefore less sensitive to single outliers than the envelope floods.

While Figure 4 shows the height of the qRECs and RECs for mesoscale catchments of 1,000 km^2 in Europe, Figure 5 shows their slopes, which is the same for both envelope and quasi-envelope curves. These slopes measure how different small and large catchments are in terms of record specific discharges. Large slopes (dark colors in Figure 5) indicate that small catchments produce specific discharges that are much larger than in large catchments. Small slopes (light colors in Figure 5) indicate that the record specific discharges in small catchments are not significantly larger than in large catchments (e.g., a slope of 0 indicates no difference). Slopes of RECs vary from 0 to −1 across European regions and larger negative values appear more frequently in Southern Europe than in Northern Europe.

This may be interpreted by having floods produced by different precipitation types in catchments of different size, that is, very intense and localized convective precipitations in small catchments and less intense and widespread frontal events in large catchments. The Mediterranean region is characterized by enhanced convection, compared with the rest of Europe, and one would therefore expect very high record flood events in small Mediterranean catchments (e.g., flash floods), meaning steeper envelope curves. Where floods for both small and large catchments are produced by the same type of precipitation, or where convective and frontal precipitation intensities are similar, one would expect smaller slopes of the envelope curve, which is what we observe in Central and Northern Europe. Also, when snowmelt is the dominant flood generating process, such as in North-Eastern Europe, one would expect negligible differences between catchments of different sizes because temperature dynamics occur in a relatively uniform way at very large spatial scales (which is confirmed by the color patterns in Figure 5).

Local characteristics (e.g., massive river regulation systems, local topography and properties of flood database) may influence the estimate of the REC slope and appear in as a local discontinuity in Figure 5, compared to the larger-scale patterns. However, these cases are limited in number and their in-depth analysis goes beyond the scope of this study.

The RECs, as characterized by Figures 4 and 5, identify the "maximum of maxima" (or almost the maximum, for the quasi-envelope curves) and indicate the flooding potential across the continent. They clearly depend on the amount of observations from which these maxima are taken from. Figure 6a shows the number of station years of data available per tile and per reference area (1,000 km^2) in Europe. Where the station density is larger (see Figure 1), so is the station-year density. Data availability in the central and western part of Europe is much larger (from 60 and up to 600 observations per 1,000 km^2) than in regions of southern, eastern and northern Europe (less than 30 observations per 1,000 km^2). This however does not translate directly into the amount of information actually available for the construction of the envelope curves. In fact, where observations come from geographically contiguous sites, one would expect that, in many cases, individual flood events are recorded more than once (i.e., they are observed at different sites), and all observations cannot be considered as independent
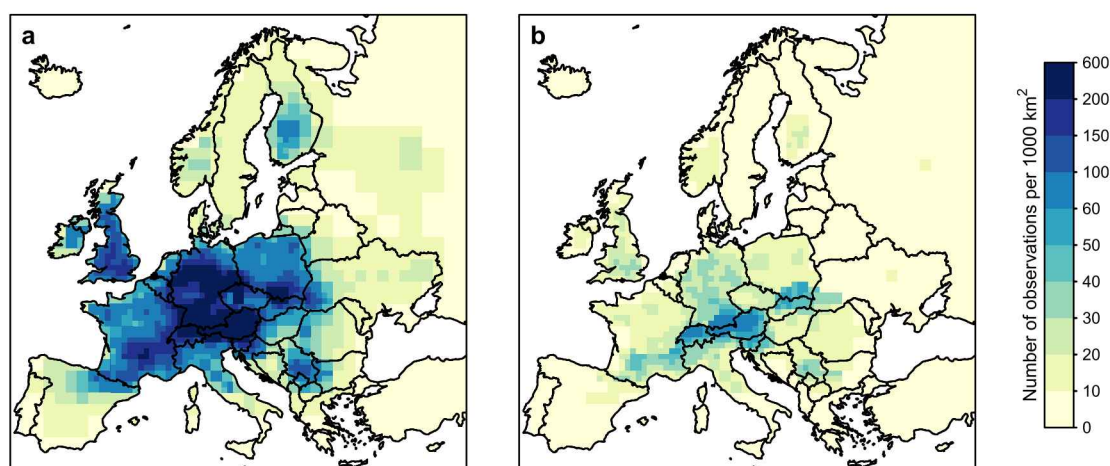
Figure 6. (a) Density of observations and (b) density of effective observations expressed as number of station-years per 1,000 km^2. The size of the tiles is shown in Figure 3a.

information. This is particularly important when an estimate of the exceedance probability (or, equivalently, the return period) associated with the RECs is sought.

In order to estimate the amount of independent information available for the construction of the RECs, we estimate the effective number of station years for each pixel with the procedure and assumptions described in Section 2.3, which accounts for the cross-correlation between observations at different sites. Figure 6 shows the dramatic difference between the available flood data (Figure 6a) and the estimate of the actual information contained in the data (Figure 6b). Even though their spatial patterns are similar, Figure 6b indicates that the amount of information for the construction of envelope curves is less heterogeneous than what one may think based on data availability only. In less densely gauged areas (i.e., areas of southern and north-eastern Europe) in fact, the average distance among the gauges is larger and the flood timeseries are less cross-correlated than in densely gauged areas. This results in the number of effective observations being very close to the total number of observations in these regions. In densely gauged areas instead (i.e., central and western Europe), there is a substantial reduction of the amount of independent information due to the cross-correlation of the timeseries. Here, the number of effective observations is typically between 20 and 60 per 1,000 km^2. There is therefore a tradeoff between the number of sites in each tile and the average distance between these sites that the effective number of station years acknowledges.

From the effective number of observations we estimate the exceedance probability associated with the REC in each of the tiles (Section 2.3, Equation 3), which is represented in Figure 7 in terms of equivalent return period. Lighter (darker) colors indicate less (more) effective observations, and therefore larger (lower) return periods associated with the RECs. The number of available observations in each tile (Figure 6a; also determined by the tile size in Figure 3a) and their cross correlation (Figure 2) have an effect on the resulting estimate of (effective number of observations and therefore of) exceedance probability. Figure 7 shows that the order of magnitude of the return period associated with the RECs is thousands of years in most regions, indicating a similar information content among the tiles of different sizes (as noted for Figure 6b in terms of effective observation density). The return period associated with the RECs is lowest (500–2,000 years) in the central-eastern and Atlantic regions due to the stronger cross-correlation of flood series for nearby gauges (Figures 2b and d), compared to other regions. This is also visible in the reduction of the number of effective observations in Figure 6b. The return period of qREC is not significantly different from that REC given that, by construction, the number of (effective) observations above the qREC is very small compared to the number of effective observations in each tile.

We finally analyse the relationship between the qREC and REC parameters and the number of effective observations and the average catchment size in the region (Figure 8). Points in Figure 8 correspond to 200 km tiles and their colours refer to five hydroclimatic regions in Figure 3c: Atlantic, Alpine, Mediterranean, Central-Eastern and North-Eastern. The tiles are assigned to hydroclimatic regions according to the location of their respective centres.
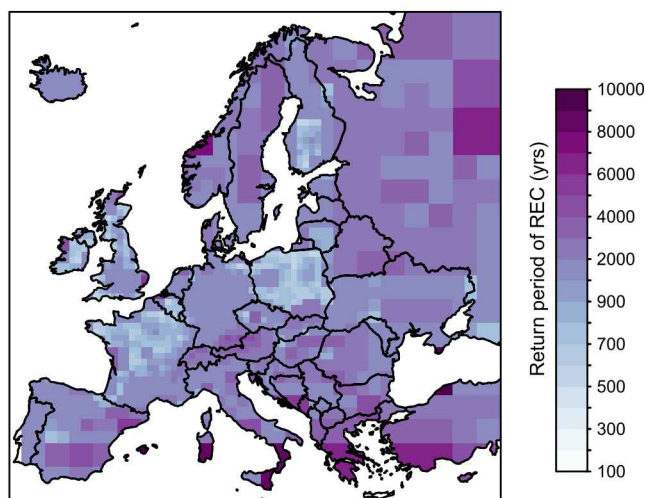
Figure 7. Map of the return periods associated with the discharge of the regional envelope curves of Figure 4b. The size of the tiles is shown in Figure 3a.

Figures 8a and 8b suggest that, while the envelope flood appears to be positively correlated with the number of effective observations, this correlation is less evident for the quasi-envelope flood. This indicates that this latter indicator is less dependent on the number of observations. The slope of the RECs is dispersed for low numbers of effective observations and it appears to converge to values between −0.3 and −0.5 for regions with increasing numbers of effective observations (Figure 8c). Differences among the five hydroclimatic regions are also visible. Tiles in the Alpine and Mediterranean (North-Eastern and Atlantic) areas have the highest (lowest) envelope and quasi-envelope floods and steepest (least steep) RECs, as also observed in Figures 4 and 5. Figure 8d indicates that there is no correlation between the REC slope and the average size of the catchments with outlets falling within each tile. Figure 8 clearly shows the advantage of qREC versus REC and allows to better compare the results in this study to what obtained in other studies, thus facilitating comparative hydrology.

4. Summary and Conclusions

This study presents an overview of the flooding potential in Europe, summarizing and illustrating the magnitude of record floods and their dependence on catchment size. The analysis is based on the most updated and comprehensive data set of European floods. The main outcomes of the study are summarized below.

1. We propose a reference framework for obtaining RECs that enables objective and comparable estimates of the expected megaflood magnitudes in large and different hydroclimatic regions. The innovative aspects of the method include the identification of regions of variable size according to the amount of available observations, the quasi-envelope curve (qREC) and flood as a more stable indicator of flooding potential in a given region compared to their traditional counterparts (i.e., envelope curve and flood).

2. We provide the parameters of RECs and qRECs for all regions in Europe, in terms of their slope and intercept for a representative catchment size of 1,000 km². Our results show that the parameters of the envelope curves vary substantially across hydroclimatic regions. The envelope flood is highest in Mediterranean and Alpine areas and lowest in central-eastern Europe. The quasi-envelope flood shows similar although smoother patterns. The slope appears higher in southern Europe than in Northern Europe. These differences across Europe indicate that some regions are more susceptible to extreme events than others and are explained by steeper landscape in mountaineous regions and localized short duration storms producing large floods in small catchments in the Mediterranean, whose intensities are larger than in other parts of Europe.

3. We provide an overview of the amount of information on record floods that is available in Europe for the construction of RECs and assess the exceedance probability of the largest observed European floods based on the probabilistic interpretation of RECs by Castellarin et al. (2005) and Castellarin (2007). We show that the RECs obtained for different regions of Europe with the proposed framework are associated with a similar amount of independent information content and a comparable exceedance probability. These findings are conditional on the assumption of homogeneous regions in terms of index flood hypothesis and that the index flood scales with catchment area.

The advantage of the proposed approach, compared to local and regional studies, is that it allows for an objective and more stable estimation of the REC parameters that is coherent across all regions of Europe. In fact, the method is not sensitive to single outliers (through the qREC) nor to the spatial variability in the density of stations. This latter is accounted for by adapting the size of the tiles so that each of them is associated by a comparable amount of independent information. The method is also based on a very simple and traditional tool (the envelope curves) and has limited data requirements compared to more complex model-based methods. These characteristics make the method suitable for large-scale applications and it can be easily applied to other regions in the world.

The spatial variability of the REC parameters is here analyzed and presented for the first time across the entire European continent. The resulting maps are a ready-to-use tool for easily characterizing the flooding potential and expected magnitude of severe floods ("megafloods") for a given catchment in Europe. Such continental
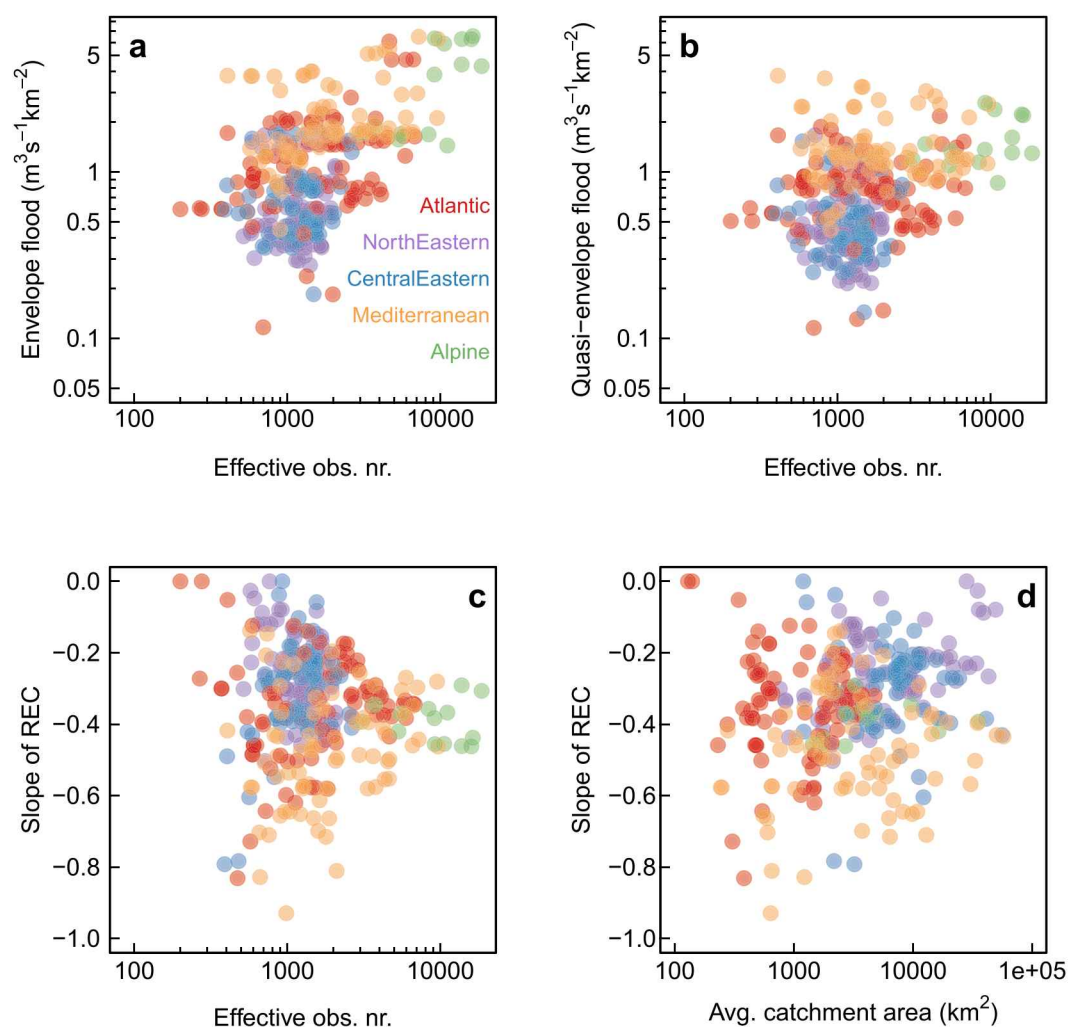
Figure 8. (a) Envelope flood versus number of effective observations; (b) quasi-envelope flood versus number of effective observations; (c) slope versus number of effective observations; (d) slope of regional envelope curve versus average catchment area of catchments with outlets within each tile. Colors refer to five European macro regions in Figure 3c. Each point refers to a 200 km tile.

assessments that go beyond regional or national borders are especially relevant for megafloods because of the limited data available (Bertola et al., 2023). This tool could also be used to learn from other similar catchments in other parts of the continent to develop possible future scenarios of extreme flooding (Bertola et al., 2023).

In conclusion, RECs are effective tools to characterize the flooding potential across large and morphologically and climatically heterogeneous geographical regions, and could complement traditional regional flood frequency analyses. We hope that the provided framework, as well as the maps of REC parameters for Europe, can be helpful in practice for flood risk managers in estimating the order of magnitude of potential extreme floods that can be expected in a region and in designing strategies against possible flooding scenarios with the ultimate goal to avoid surprising damages and losses.

Data Availability Statement

The flood discharge data used in this paper can be obtained from the Supplement of Bertola et al. (2023) and are accessible at Bertola (2024).

References

Amadio, M., Scorzini, A. R., Carisi, F., Essenfelder, A. H., Domeneghetti, A., Mysiak, J., & Castellarin, A. (2019). Testing empirical and synthetic flood damage models: The case of Italy. *Natural Hazards and Earth System Sciences*, *19*(3), 661–678. https://doi.org/10.5194/nhess-19-661-2019

Amponsah, W., Marra, F., Marchi, L., Roux, H., Braud, I., & Borga, M. (2020). Objective analysis of envelope curves for peak floods of European and Mediterranean flash floods. In W. Leal Filho, G. Nagy, M. Borga, P. Chávez Muñoz, & A. Magnuszewski (Eds.), *Climate change, hazards and adaptation options*. Climate Change Management. Springer.

Bertola, M. (2024). Tuwhydro/megafloods: Data and R code (R) (Version 1) [Software]. *Zenodo*. https://doi.org/10.5281/zenodo.13771956

Bertola, M., Blöschl, G., Bohac, M., Borga, M., Castellarin, A., Chirico, G. B., et al. (2023). Megafloods in Europe can be anticipated from observations in hydrologically similar catchments. *Nature Geoscience*, *16*(11), 982–988. https://doi.org/10.1038/s41561-023-01300-5

Bertola, M., Viglione, A., Lun, D., Hall, J., & Blöschl, G. (2020). Flood trends in Europe: Are changes in small and big floods different? *Hydrology and Earth System Sciences*, *24*(4), 1805–1822. https://doi.org/10.5194/hess-24-1805-2020

Bertola, M., Viglione, A., Vorogushyn, S., Lun, D., Merz, B., & Blöschl, G. (2021). Do small and large floods have the same drivers of change? A regional attribution analysis in Europe. *Hydrology and Earth System Sciences*, *25*(3), 1347–1364. https://doi.org/10.5194/hess-25-1347-2021

Blöschl, G., Hall, J., Parajka, J., Perdigão, R. A. P., Merz, B., Arheimer, B., et al. (2017). Changing climate shifts timing of European floods. *Science*, *357*(6351), 588–590. https://doi.org/10.1126/science.aan2506

Blöschl, G., Hall, J., Viglione, A., Perdigão, R. A. P., Parajka, J., Merz, B., et al. (2019). Changing climate both increases and decreases European river floods. *Nature*, *573*(7772), 108–111. https://doi.org/10.1038/s41586-019-1495

Carisi, F., Schröter, K., Domeneghetti, A., Kreibich, H., & Castellarin, A. (2018). Development and assessment of uni- and multivariable flood loss models for Emilia-Romagna (Italy). *Natural Hazards and Earth System Sciences*, *18*(7), 2057–2079. https://doi.org/10.5194/nhess-18-2057-2018

Castellarin, A. (2007). Probabilistic envelope curves for design flood estimation at ungauged sites. *Water Resources Research*, *43*(4), 1–12. https://doi.org/10.1029/2005WR004384

Castellarin, A., Merz, R., & Blöschl, G. (2009). Probabilistic envelope curves for extreme rainfall events. *Journal of Hydrology*, *378*(3–4), 263–271. https://doi.org/10.1016/j.jhydrol.2009.09.030

Castellarin, A., Vogel, R. M., & Matalas, N. C. (2005). Probabilistic behavior of a regional envelope curve. *Water Resources Research*, *41*(6), 1–13. https://doi.org/10.1029/2004WR003042

Castellarin, A., Vogel, R. M., & Matalas, N. C. (2007). Multivariate probabilistic regional envelopes of extreme floods. *Journal of Hydrology*, *336*(3–4), 376–390. https://doi.org/10.1016/j.jhydrol.2007.01.007

Creager, W. P., Justin, J. D., & Hinds, J. (1966). *Engineering for dams* (Vol. 1, pp. 99–140). John Wiley.

Crippen, J. R., & Bue, C. D. (1977). *Maximum flood flows in the con-terminous United States* (Vol. 1887). U.S. Geological. Survey. Water Supply Paper.

Dalrymple, T. (1960). *Flood frequency analyses* (pp. 1543–A). U.S. Geological. Survey. Water Supply Paper.

Douglas, E. M., & Vogel, R. M. (2006). Probabilistic behavior of floods of record in the United States. *Journal of Hydrologic Engineering*, *11*(5), 482–485. https://doi.org/10.1061/(asce)1084-0699(2006)11:5(482)

European Union. (2007). Directive 2007/60/EC of the European parliament and of the council of 23 October 2007 on the assessment and management of flood risks. *Official Journal of the European Union L*, *288*, 27–34.

Farmer, W. H., Kiang, J. E., Feaster, T. D., & Eng, K. (2019). *Regionalization of surface-water statistics using multiple linear regression*. U.S. Geological Survey Techniques and Methods (p. 40). https://doi.org/10.3133/tm4A12

Fekete, A., & Sandholz, S. (2021). Here comes the flood, but not failure? Lessons to learn after the heavy rain and pluvial floods in Germany 2021. *Water*, *13*(21), 3016. https://doi.org/10.3390/w13213016

Fuller, W. E. (1914). Flood flows. *Transactions of the American Society of Civil Engineers*, *77*(1), 564–617. https://doi.org/10.1061/taceat.0002552

Gathen, M., Welle, K., Jaenisch, M., Kasapovic, A., Rommelspacher, C., Novosel, S., et al. (2022). Are orthopaedic surgeons prepared? An analysis of severe casualties from the 2021 flash flood and mudslide disaster in Germany. *European Journal of Trauma and Emergency Surgery*, *48*(5), 4233–4241. https://doi.org/10.1007/s00068-022-01967-2

Gaume, E., Bain, V., Bernardara, P., Newinger, O., Barbuc, M., Bateman, A., et al. (2009). A compilation of data on European flash floods. *Journal of Hydrology*, *367*(1–2), 70–78. https://doi.org/10.1016/j.jhydrol.2008.12.028

Gumbel, E. J. (1941). The return period of flood flows. *The Annals of Mathematical Statistics*, *12*(2), 163–190. https://doi.org/10.1214/aoms/1177731747

Guse, B., Thieken, A. H., Castellarin, A., & Merz, B. (2010). Deriving probabilistic regional envelope curves with two pooling methods. *Journal of Hydrology*, *380*(1–2), 14–26. https://doi.org/10.1016/j.jhydrol.2009.10.010

Herschy, R. W. (2002). The world's maximum observed floods. *Flow Measurement and Instrumentation*, *13*(5–6), 231–235. https://doi.org/10.1016/S0955-5986(02)00054-7

Jarvis, C. S. (1926). Flood flow characteristics. *Transactions of the American Society of Civil Engineers*, *88*(1), 985–1032. https://doi.org/10.1061/taceat.0003607

Lun, D., Viglione, A., Bertola, M., Komma, J., Parajka, J., Valent, P., & Blöschl, G. (2021). Characteristics and process controls of statistical flood moments in Europe – A data-based analysis. *Hydrology and Earth System Sciences*, *25*(10), 5535–5560. https://doi.org/10.5194/hess-25-5535-2021

Marchetti, G. (1955). Sulle massime portate di piena osservate nei corsi d'acqua italiani a tutto il 19 53, G. *Genio Civ.*, *93*(3–4).

Marchi, L., Borga, M., Preciso, E., & Gaume, E. (2010). Characterisation of selected extreme flash floods in Europe and implications for flood risk management. *Journal of Hydrology*, *394*(1–2), 118–133. https://doi.org/10.1016/j.jhydrol.2010.07.017

Matalas, N. C., & Langbein, W. B. (1962). Information content of the mean. *Journal of Geophysical Research*, *67*(9), 3441–3448. https://doi.org/10.1029/jz067i009p03441

Merz, B., Blöschl, G., Vorogushyn, S., Dottori, F., Aerts, J. C., Bates, P., et al. (2021). Causes, impacts and patterns of disastrous river floods. *Nature Reviews Earth & Environment*, *2*(9), 592–609. https://doi.org/10.1038/s43017-021-00195-3

Mimikou, M. (1984). Envelope curves for extreme flood events in Northwestern and Western Greece. *Journal of Hydrology*, *67*(1–4), 55–66. https://doi.org/10.1016/0022-1694(84)90232-4

Parrett, C., Veilleux, A., Stedinger, J. R., Barth, N. A., Knifong, D. L., & Ferris, J. C. (2011). *Regional skew for California, and flood frequency for selected sites in the Sacramento-San Joaquin River Basin, based on data through water year 2006*. US Geological Survey.

Slater, L., Villarini, G., Archfield, S., Faulkner, D., Lamb, R., Khouakhi, A., & Yin, J. (2021). Global changes in 20-year, 50-year, and 100-year river floods. *Geophysical Research Letters*, *48*(6), e2020GL091824. https://doi.org/10.1029/2020gl091824

Stedinger, J. R. (1983). Estimating a regional flood frequency distribution. *Water Resources Research*, *19*(2), 503–510. https://doi.org/10.1029/wr019i002p00503

Tasker, G. D., & Stedinger, J. R. (1989). An operational GLS model for hydrologic regression. *Journal of Hydrology*, *111*(1–4), 361–375. https://doi.org/10.1016/0022-1694(89)90268-0

Viglione, A., Castellarin, A., Rogger, M., Merz, R., & Blöschl, G. (2012). Extreme rainstorms: Comparing regional envelope curves to stochastically generated events. *Water Resources Research*, *48*(1). https://doi.org/10.1029/2011wr010515